FISEVIER

Contents lists available at ScienceDirect

Chemical Physics Letters

journal homepage: www.elsevier.com/locate/cplett



Research paper

Optical and photodynamic properties of carbon/TiO₂ hybrid dots in different nanoscale configurations



Nengyu Pan^{a,1}, Peter A. Okonjo^{b,1}, Ping Wang^a, Yongan Tang^c, Ya-Ping Sun^{a,*}, Liju Yang^{b,*}

- ^a Department of Chemistry and Laboratory for Emerging Materials and Technology, Clemson University, Clemson, SC 29634, USA
- b Department of Pharmaceutical Sciences, Biomanufacturing Research Institute and Technology Enterprise, North Carolina Central University, Durham, NC 27707, USA
- ^c Department of Mathematics and Physics, North Carolina Central University, Durham, NC 27707, USA

HIGHLIGHTS

- Carbon dots (CDots) exploit unique properties of small carbon nanoparticles;
- Carbon/semiconductor hybrid dots substantially expand the CDots platform;
- Carbon/TiO2 dots in different compositions/configurations can be designed and prepared;
- The hybrid dots can be explored for different photoexcited state properties;
- The hybrid dots can serve as effective photodynamic antibacterial agents.

ABSTRACT

Carbon/TiO₂ hybrid dots with the general configuration of nanoscale carbon domains incorporated with TiO₂ nanoparticles of different sizes (8 and 25 nm in diameter) were prepared and characterized, and their optical and photodynamic properties were studied. The properties were found to be affected dramatically by the relative sizes and configurations of the nanoscale carbon domains and TiO₂ nanoparticles in the hybrid dots, as reflected by the observed major difference in their photodynamic inactivation of bacteria under visible light. Mechanistic implications of the results are discussed.

1. Introduction

Carbon "quantum" dots or carbon dots (CDots) [1,2], generally defined as small carbon nanoparticles with various surface passivation schemes [3,4], are analogous to core-shell nanostructures (Fig. 1), each with a carbon nanoparticle core and a thin shell of soft materials (organic or biological species) for the particle surface passivation function. Ever since their finding [1,2], CDots have attracted a tremendous amount of attention, as reflected by the large and ever increasing number of publications in the literature on both fundamental and technological developments [4–15].

Among widely pursued applications of CDots have been those that exploit their strong optical absorptions over a broad spectral region and their photoexcited state properties and processes [3,4,9], including photodynamic inactivation of microbials [14,15]. Beyond neat CDots, the core carbon nanoparticles in CDots are structurally compatible with other molecular and nanoscale materials, namely that the carbon nanoparticles can be modified in various configurations and/or compositions by other materials such as traditional dyes or conventional

nanoscale semiconductors like TiO_2 [9,16–25]. The corresponding dots with the modified core nanoparticles are referred to as carbon-based hybrid nanostructures or simply hybrid CDots, and those with the core nanoparticles composed of carbon and TiO_2 may be denoted generally as C/TiO_2 -Dots (Fig. 1) [18]. In fact, the incorporation of nanoscale TiO_2 into CDots has been particularly popular, mostly for the purpose of improving photocatalytic energy conversions from those achieved by neat CDots as photocatalysts [9,19–25].

Within the family of C/TiO₂-Dots (Fig. 1), which share a common feature of the core nanoparticles composed of nanoscale carbon and ${\rm TiO}_2$, there are different members of significantly different dot fine structures and properties due to variations in the sizes of the incorporated ${\rm TiO}_2$ nanoparticles, the relative dimensions and arrangements between the nanoscale carbon and ${\rm TiO}_2$ domains in the core nanoparticles, and also the organic species for the surface passivation function (Fig. 1). These variations and differences among members of C/TiO₂-Dots can have dramatic effects on their optical properties and redox characteristics [18], and by extension also on their photodynamic properties.

E-mail addresses: syaping@clemson.edu (Y.-P. Sun), lyang@nccu.edu (L. Yang).

^{*} Corresponding authors.

¹ Authors made equal contributions.



Fig. 1. Cartoon illustrations on one of neat CDots (upper left), C/TiO_2 hybrid dots with small TiO_2 nanoparticles (upper right), and C/TiO_2 hybrid dots in which a larger TiO_2 nanoparticle is "decorated" with various nanoscale surface-functionalized carbon domains (lower).

In this study, C/TiO $_2$ -Dots containing TiO $_2$ nanoparticles of different sizes were prepared and characterized. In these hybrid dots, the relative sizes and configurations of the nanoscale carbon domains and TiO $_2$ nanoparticles were different, corresponding to very different photoexcited state properties and related photodynamic effects, as observed experimentally. The mechanistic implications of the results are discussed, so are the potential and values of the selected high-performance C/TiO $_2$ dot configuration in photodynamic inactivation of microbials and related applications.

2. Results and discussion

Carbon/TiO2 hybrid dots of different sizes, corresponding to different carbon and TiO2 relative domain sizes and arrangements in the core nanoparticles of the dots (Fig. 1), were prepared by using precursor mixtures of pre-existing TiO2 nanoparticles and organic molecules for thermal carbonization processing under various processing conditions. The TiO₂ nanoparticles of average diameter about 8 nm were prepared from titanium ethoxide in a hydrothermal processing, as reported previously [18], and those of average diameter around 25 nm (according to X-ray powder diffraction peak broadening and Scherrer equation) were harvested from commercially supplied colloidal TiO2 (Deguasa P25) in a procedure involving vigorous sonication for the dispersion in ethanol and then gravimetric fractionation. These TiO2 nanoparticles of small and larger in average sizes were dispersible in aqueous or polar organic media, allowing the desired solution-phase mixing with selected organic molecules for the targeted precursor mixtures.

Oligomeric polyethylene glycol of average molecular weight ~ 1500 (PEG $_{1500}$) was used as both the carbon source and the surface

functionalization agent for the targeted carbon/TiO₂ hybrid dots. The precursor mixture was prepared such that the TiO₂ nanoparticles were well dispersed in PEG₁₅₀₀ for the microwave-assisted thermal processing. The hybrid dots prepared from the small TiO₂ nanoparticles were the same as those reported previously [18], denoted as PEG-C/TiO₂ (8nm)-Dots_i with i=1 and 2 for the dots containing 71 wt% and 31 wt% of TiO₂ in the core nanoparticles, respectively.

For the hybrid dots with the larger TiO_2 nanoparticles, denoted as PEG-C/ TiO_2 ($^{(25nm)}$ -Dots, similar but somewhat more vigorous processing conditions were applied. The experimental procedures included a number of repeated processing cycles, each of which included microwave-assisted thermal carbonization and then cooling to avoid burning the sample. The hybrid dot structure targeted in the processing was a larger TiO_2 nanoparticle decorated with nanoscale carbon domains, whose surfaces were passivated by the remaining PEG moieties that survived the carbonization processing conditions (Fig. 1). With the PEG moieties on the surface, the hybrid dots were expected to be readily soluble (dispersed very well), so the aqueous soluble fraction of the reaction mixture was harvested and then cleaned to obtain the PEG-C/ TiO_2 ($^{(25nm)}$ -Dots as a colored aqueous solution. Its optical absorption spectrum is similar to those of PEG-C/ TiO_2 ($^{(8nm)}$ -Dots, as compared in Fig. 2.

For the introduction of amino groups into the surface passivation moieties in the hybrid dots, oligomeric polyethylenimine (average molecular weight ${\sim}600$) was used in combination with PEG₁₅₀₀ in the precursor mixture with the larger TiO₂ nanoparticles for the same microwave-assisted carbonization processing. The resulting hybrid dots, denoted as PEI&PEG-C/TiO₂ $^{(25nm)}$ -Dots, were similarly harvested as a colored aqueous solution. Its optical absorption spectrum is rather similar to that of the hybrid dots without PEI, as also compared in Fig. 2. The rather similar optical absorption and fluorescence emission spectra among the hybrid dots with TiO₂ nanoparticles of different sizes were as expected, because of the spectra (profiles, not quantum yields) associated only with the organic passivated nanoscale carbon domains in the dot structures, little affected by the presence of TiO₂ nanoparticles (transparent in the visible spectrum).

The dot sample was characterized by atomic force microscopy (AFM) and transmission electron microscopy (TEM). Results from both microscopy methods suggested larger average dot sizes than 25 nm (Fig. 3), which might be attributed at least in part to the decoration of individual larger TiO_2 nanoparticle by nanoscale carbon domains in the carbonization processing (Fig. 1).

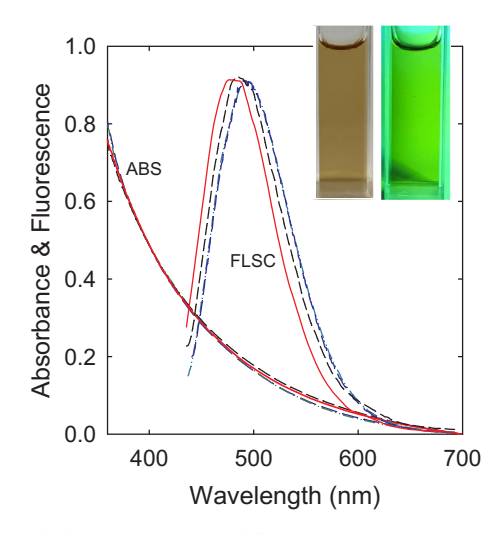


Fig. 2. Optical absorption (ABS) and fluorescence (FLSC) spectra of PEG-C/ $TiO_2^{(8nm)}$ -Dots₁ (— —), PEG-C/ $TiO_2^{(8nm)}$ -Dots₂ (- • - • -), PEG-C/ $TiO_2^{(25nm)}$ -Dots (— —), and PEI&PEG-C/ $TiO_2^{(25nm)}$ -Dots (——) in aqueous solutions. Inset: Photos for an aqueous solution of PEI&PEG-C/ $TiO_2^{(25nm)}$ -Dots under ambient light (left) and near-UV light (around 370 nm, right).

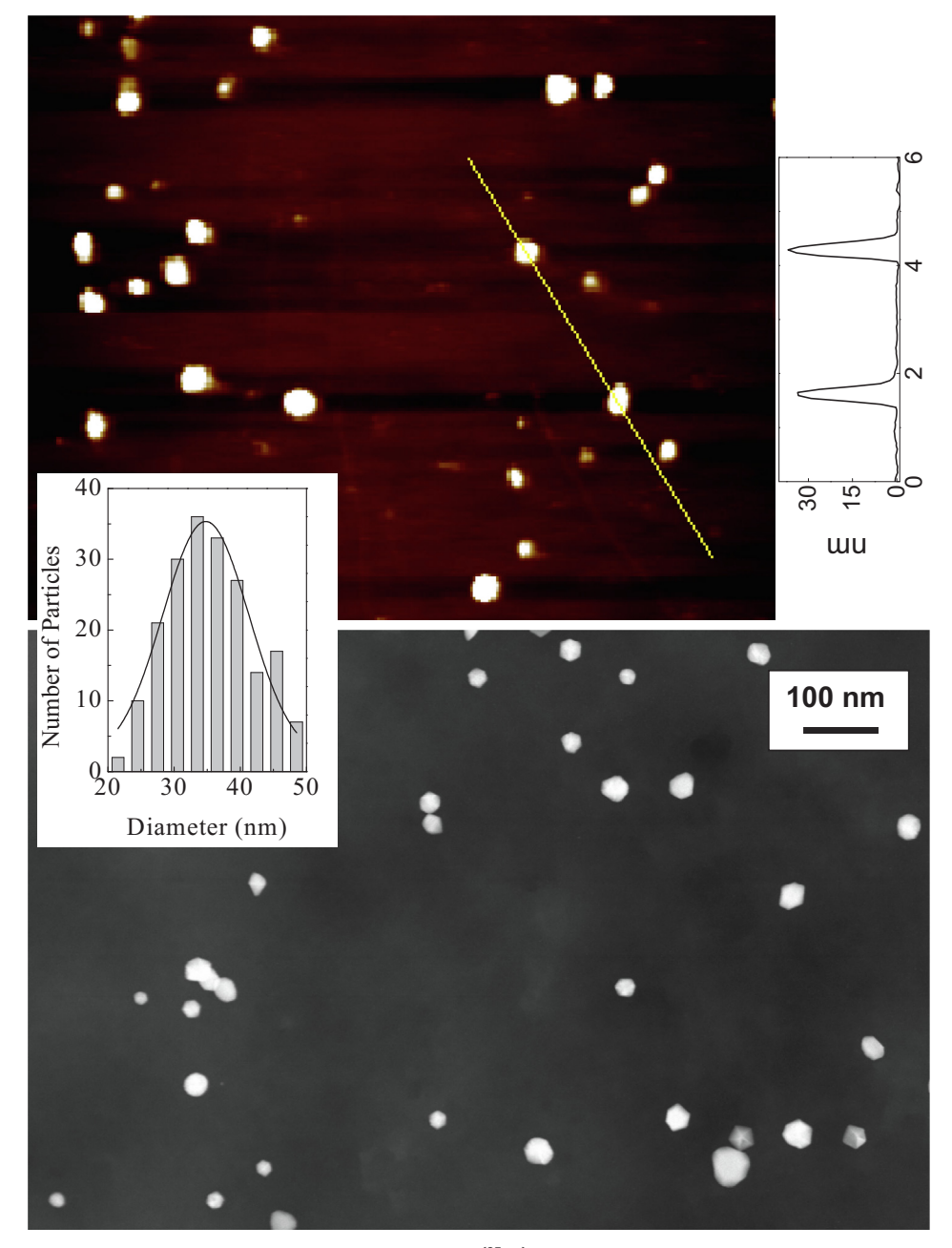


Fig. 3. Representative AFM (upper) and TEM (lower) images of PEI&PEG-C/TiO₂ (25nm)_Dots. Inset: Statistical analysis of dot sizes based on multiple AFM images.

There were fluorescence emissions from PEG-C/TiO $_2^{(25nm)}$ -Dots and PEI&PEG-C/TiO $_2^{(25nm)}$ -Dots with excitations in the visible (Fig. 2), similar to those found in PEG-C/TiO $_2^{(8nm)}$ -Dots $_i$ [18], but the observed quantum yields were only 0.5–1%, significantly lower than those of CDots without any TiO $_2$ [18,26]. Since TiO $_2$ nanoparticles are not absorptive in the visible, the observed fluorescence emissions could only be associated with the nanoscale carbon domains (absorptive in the visible, Fig. 2) in the hybrid dots. Thus, the much weaker fluorescence emissions could be attributed to the intra-dot quenching effects by the attached TiO $_2$ due to electron transfers, similar to those known in dyesensitized TiO $_2$ systems [27–29], with nanoscale carbon domains in the hybrid dots serving the dye function for the harvesting of visible photons.

Mechanistically, the sensitization of the small (8 nm) and larger (25 nm) ${\rm TiO_2}$ nanoparticles by photoexcited carbon domains in their corresponding hybrid dot structures should largely be the same, but consequences of the sensitization in the hybrid dots with the small and

larger ${\rm TiO_2}$ nanoparticles were very different, as reflected by the completely different outcomes in their photodynamic inactivation of bacteria.

PEG-C/TiO $_2$ (8nm)-Dots $_i$ (i=1 and 2 containing 71 wt% and 31 wt% of TiO $_2$, respectively) were evaluated for their visible light-activated antibacterial activities against the laboratory model bacteria *Bacillus subtilis*. Shown in Fig. 4 are results in terms of the viable cell reduction after the cells were treated with the hybrid dots at various concentrations under visible light (400–780 nm broad-band LED) for 2 h. The concentrations, from 0.02 to 0.2 mg/mL (Fig. 4), are carbon-equivalent concentrations based on the carbon content in the core nanoparticles of the hybrid dots, because the nanoscale carbon domain should be solely responsible for the visible light excitation. The two PEG-C/TiO $_2$ (8nm)-Dots $_i$ (i=1 and 2) both exhibited only moderate antibacterial activities towards *B. subtilis*, killing 0.5–2.5 logs of cells with the dot concentration increased from 0.02 to 0.2 mg/mL. However, the trend shown in Fig. 4 on the concentration dependence suggested rather limited rooms

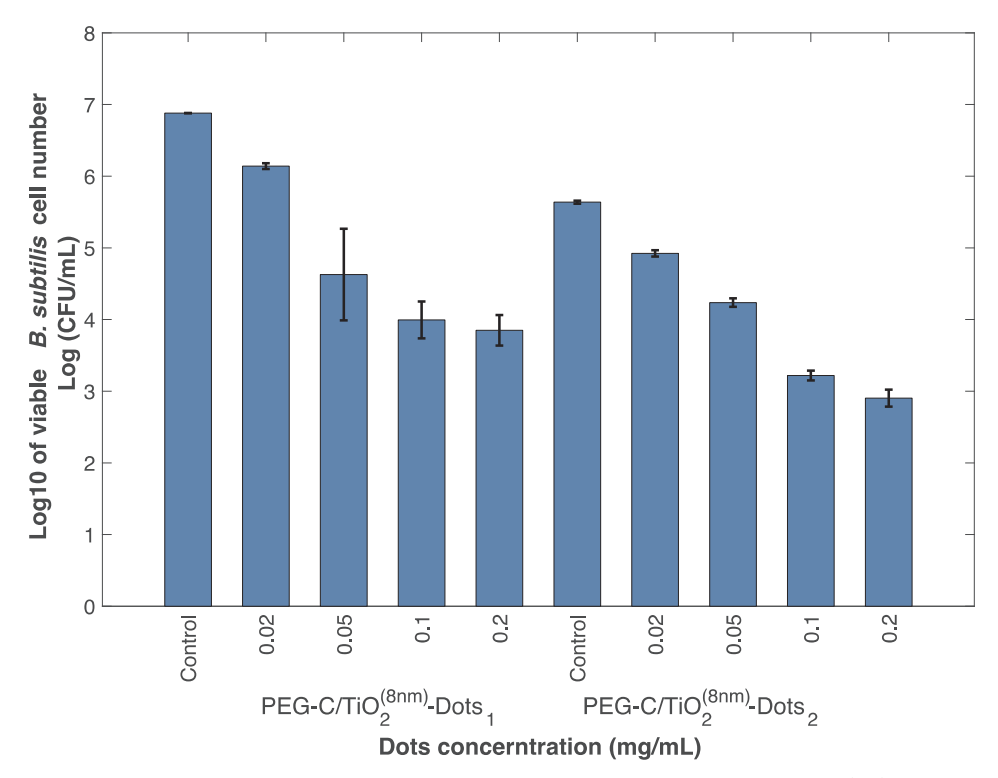


Fig. 4. Logarithmic viable cell numbers of *B. subtilis* in untreated control samples and the samples treated with PEG-C/TiO₂^(8nm)-Dots₁ and PEG-C/TiO₂^(8nm)-Dots₂ at concentrations ranging from 0.02 mg/mL to 0.2 mg/mL for 2 h under illumination of a 60 W-equivalent day-light LED.

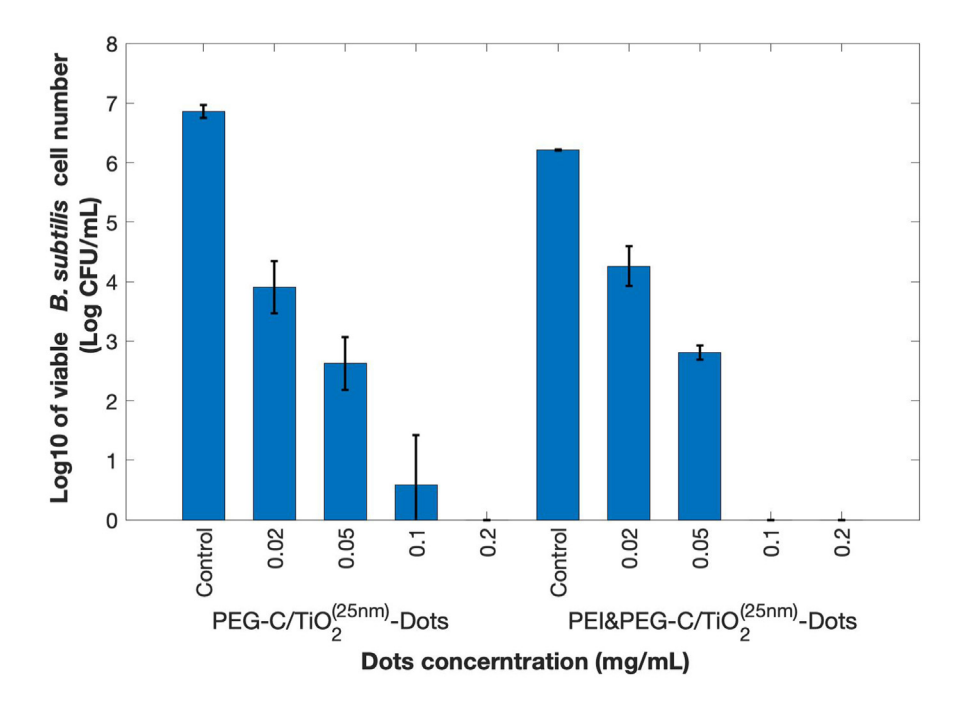
for further increasing the antibacterial efficiency with even higher dot concentrations.

The larger TiO₂ nanoparticles in PEG-C/TiO₂^(25nm)-Dots and PEI& PEG-C/TiO₂^(25nm)-Dots could apparently enhance the antibacterial functions significantly. Shown in Fig. 5 are viable cell reduction results of these hybrid dots obtained with the same experimental protocol against *B. subtilis* cells. Upon the treatment with both dot samples, the viable cell number of *B. subtilis* reduced in a concentration-dependent manner. For the treatments with PEG-C/TiO₂^(25nm)-Dots at concentrations (again carbon-equivalent concentrations for the nanoscale carbon domains in the cores of the hybrid dots, Fig. 1) of 0.02, 0.05, and 0.1 mg/mL under visible light for 2 h, the viable cell number reduced by 2.95, 4.23, and 6.29 log, respectively; and with PEI&PEG-C/TiO₂^(25nm)-Dots under the same conditions, the viable cell number reductions were 1.95, 3.4 and 6.21, respectively.

The photodynamic inactivation results on the much better performance of the hybrid dots with larger TiO2 nanoparticles are counterintuitive for several reasons. Because of the larger ${\rm TiO_2}$ nanoparticles and therefore larger hybrid dot sizes, their corresponding solutions are subject to more significant light scattering effects, which could interfere with the light absorption in the photoirradiation experiments. The interference might be more pronounced for the specific hybrid dot configuration, in which the nanoscale carbon domains responsible for the light absorption are attached to the larger TiO₂ nanoparticle (Fig. 1). The overall larger hybrid dot sizes are also unfavorable in comparison with their smaller counterparts in interactions with the targeted bacterial cells. Thus, the higher performance of the larger hybrid dots must be due to mechanistic reasons associated with the photoexcited states and related photodynamic properties. In all of the C/TiO2 hybrid dots in this study, upon photoexcitation with the light absorption by the nanoscale carbon domains, the TiO2 nanoparticles in the same hybrid dot structures are sensitized, similar to what is known in dye-sensitized TiO₂ systems [27-29]. Consequently, both the photoexcited carbon domains (those survived the quenching by TiO2) and the sensitized TiO₂ nanoparticles could induce photodynamic effects. The former

must be similar between the hybrid dots with small and larger ${\rm TiO_2}$ nanoparticles, but the latter very different in terms of the photodynamic effects actually resulting in the inactivation of bacteria. In the hybrid dot structures, the small ${\rm TiO_2}$ nanoparticles are enclosed by carbon shells surface-functionalized with organic moieties, so that their photodynamic generation of ROS (reactive oxygen species) could be hindered and/or the produced ROS in their lifetimes could not reach and act on the bacteria. On the other hand, the larger ${\rm TiO_2}$ nanoparticles in the hybrid dot structures are much more exposed (Fig. 1), capable of the effective photodynamic inactivation, as observed experimentally. The combined photodynamic effects of the photoexcited carbon domains and their sensitized larger ${\rm TiO_2}$ nanoparticles make the larger ${\rm C/TiO_2}$ hybrid dots highly effective visible light-activated bactericidal agents.

The results presented above and their associated mechanistic implications are highly valuable in the development of carbon-based/derived hybrid nanostructures incorporated with nanoscale semiconductors for a variety of technological applications. As discussed earlier, C/TiO2 hybrid dot structures have been pursued more extensively for their serving as photocatalysts, which share most of the same photoexcited state properties and processes with photodynamic effects. For photodynamic inactivation, C/TiO2 hybrid dots offer significant advantages over traditional dye-sensitized TiO2 systems, including high photostability, efficient activation by visible light, and others in addition to the high inactivation performance due to the combined ROS generation by the photoexcited carbon domains and the sensitized TiO₂ nanoparticles. It should also be stressed that the larger TiO₂ nanoparticles are commercially available and very inexpensive, and their corresponding C/TiO2 hybrid dots can be produced facilely and efficiently, thus amenable to broad uses as effective visible/natural light-activated bactericidal agents, photocatalysts, and a versatile nanomaterials platform for other technological applications.



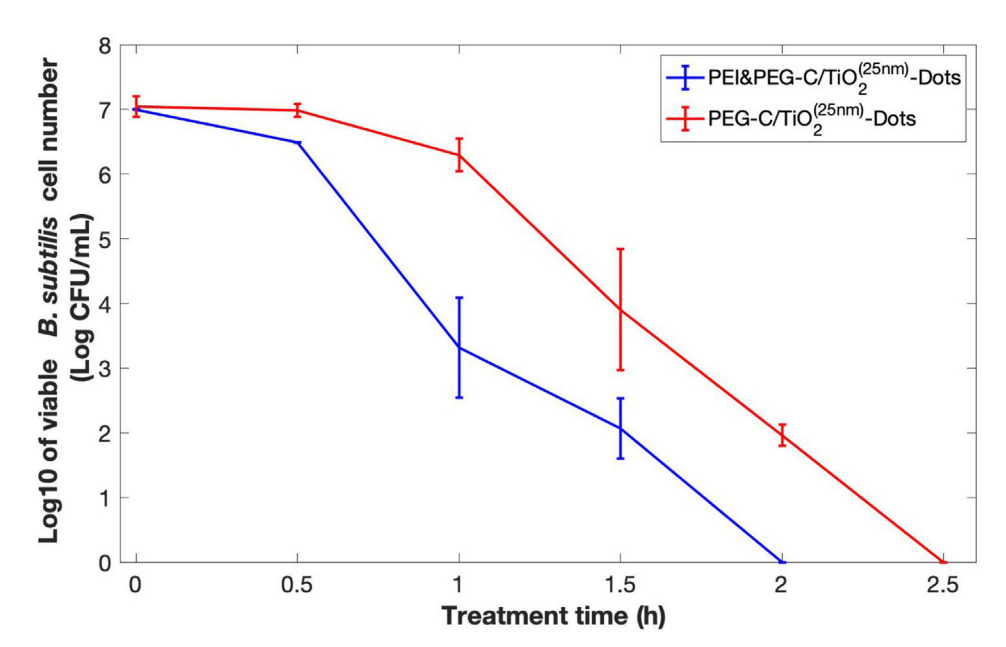


Fig. 5. (A, upper) Logarithmic viable cell numbers of *B. subtilis* in untreated control samples and the samples treated with PEG-C/TiO₂^(25nm)-Dots and PEI&PEG-C/TiO₂^(25nm) at concentrations ranging from 0.02 mg/mL to 0.2 mg/mL for 2 h under illumination of a 60 W-equivalent day-light LED. (B, lower) The logarithmic reduction in viable cell numbers of *B. subtilis* in the samples treated with 0.1 mg/mL PEG-C/TiO₂^(25nm)-Dots and PEI&PEG-C/TiO₂^(25nm)-Dots of increasing treatment time.

3. Conclusions

Carbon/TiO₂ hybrid dots with a general configuration of nanoscale carbon domains incorporated with TiO₂ nanoparticles of different sizes could be prepared by using pre-existing TiO₂ nanoparticles and organic precursors in microwave-assisted carbonization processing. The resulting hybrid dots exhibited only weak fluorescence emissions in comparison with those found in their neat counterparts without any TiO₂. The hybrid dots with TiO₂ nanoparticles of larger sizes (25 nm in average diameter) were found to be much more effective than those of small sizes (8 nm in average diameter) in the visible light-activated killing of bacterial cells. The results are rationalized such that these

larger ${\rm TiO_2}$ nanoparticles could not be enclosed by the carbon domains to hinder their photosensitized actions against the targeted bacteria, which combined with the contribution of the photoexcited carbon domains make these hybrid dots particularly effective bactericidal agents. The same understandings of the photoexcited state properties and processes may also be valuable in the development of the hybrid dots for photocatalysis and other applications.

4. Experimental section

4.1. Materials

The colloidal TiO_2 sample (Degussa P25) was purchased from Aldrich. Ethanol (> 99%) was obtained from VWR, oligomeric polyethylene glycol (PEG₁₅₀₀, average molecular weight ~1500) from Fluka, and oligomeric polyethylenimine (PEI, average molecular weight ~600) from Polysciences. Silicon carbide powders (120 Grit) were supplied by Panadyne Abrasives, and dialysis membrane tubing (molecular weight cut-off ~25,000) by Spectrum Laboratories. Water was deionized and purified by being passed through a Labconco WaterPros water purification system.

4.2. Measurement

UV/vis absorption spectra were recorded on a Shimadzu UV2501-PC spectrophotometer. Fluorescence spectra were collected on a Horiba Jobin-Yvon emission spectrometer equipped with a 450 W xenon source, Gemini-180 excitation (1 mm slit) and Triax-550 emission (1 mm slit) monochromators, and a photon counting detector (Hamamatsu R928P PMT at 950 V). Powder X-ray diffraction measurements were performed on a Rigaku Ultima IV X-ray diffractometer with Cu K α radiation ($\lambda = 1.5418$ Å) at 25 °C. Transmission electron microscopy (TEM) images were acquired on a Hitachi H-9500 highresolution TEM system. The TEM specimen was prepared by depositing a few drops of a dilute sample solution onto silicon-based grids, followed by the removal of solvent via evaporation. Atomic force microscopy (AFM) images were acquired in the acoustic AC mode on a Molecular Imaging PicoPlus AFM system equipped with a multipurpose scanner and a NanoWorld point probe NCH sensor. The height profile analysis was assisted by using SiPIP software distributed by Image Metrology.

4.3. $PEG-C/TiO_2^{(25nm)}$ -Dots

Commercially supplied colloidal ${\rm TiO_2}$ sample (Degussa P25) was dispersed in ethanol via vigorous sonication, followed by centrifuging at 1000g to collect the supernatant as an ethanol dispersion of the harvested ${\rm TiO_2}$ nanoparticles. An aliquot of the dispersion (50 mg of ${\rm TiO_2}$) was mixed with ${\rm PEG_{1500}}$ (2 g) in a glass vial via vigorous sonication. The resulting dispersion appeared homogeneous, and from the dispersion ethanol was removed by purging with nitrogen gas to obtain the desired precursor mixture of the ${\rm TiO_2}$ nanoparticles dispersed in ${\rm PEG_{1500}}$ for the microwave-assisted thermal carbonization processing.

The glass vial containing the precursor mixture was immersed in a silicon carbide bath (about 8 cm in diameter and 2.5 cm in height, containing about 50 g silicon carbide) in a conventional microwave oven. With the oven power set at 700 W, the sample was treated with microwave irradiation for 110 s, followed by taking the sample vial out of the oven for 60 s and then re-immersing the vial in the silicon carbide bath in the microwave over for the next heating-cooling treatment cycle. The same cycle was repeated for 7 more times. Then, to the reaction mixture was added more PEG₁₅₀₀ (1 g) with ethanol for a dispersion via sonication, followed by the removal of ethanol via purging with nitrogen gas. The resulting mixture in the silicon carbide bath was treated with the above-described cycle of microwave heating at 700 W and then cooling for 11 repeats. Again, to the reaction mixture was added more PEG₁₅₀₀ (1 g) with ethanol for the same dispersion and then solvent removal, was then added respectively, followed by 5 cycles of microwave heating at 900 W and then cooling. One more addition of PEG₁₅₀₀ (1 g) and then the same processing cycles were performed to obtain the final reaction mixture. The mixture back at ambient temperature was dispersed in hot deionized water (15 mL) with sonication, and the resulting dispersion was dialyzed (molecular weight cut-off ~25,000) against fresh deionized water for 24 h to yield PEG-C/

 ${\rm TiO_2}^{(25{\rm nm})}$ -Dots as apparently a homogenous aqueous dispersion.

4.4. PEI&PEG-C/TiO₂^(25nm)-Dots

An aliquot of the same ethanol dispersion of ${\rm TiO_2}$ (50 mg) was mixed with PEI (0.5 g) and PEG₁₅₀₀ (1 g) in a glass vial with sonication to obtain a homogeneous dispersion, followed the removal of ethanol via purging with nitrogen gas. The sample vial was immersed in the silicon carbide bath for the microwave heating at 900 W and for 110 s and then cooling in 5 repeating cycles. Then, in 3 repeats, each included the addition of more PEG₁₅₀₀ (1 g) with ethanol to the reaction micture for a homogeneous dispersion, followed by the removal of ethanol, and then for the resulting mixture to be treated with the same microwave heating and then cooling cycle for 4 times. The final reaction mixture back at ambient temperature was dispersed in hot deionized water (15 mL), followed by dialysis (molecular weight cut-off ~ 25,000) against fresh deionized water for 24 h to obtain the PEG-C/TiO₂ (25nm)-Dots in apparently a homogeneous aqueous dispersion.

4.5. Visible Light-Activated antibacterial functions

B. subtilis culture was grown in 10 mL nutrient broth (Fisher Scientific, Pittsburgh, PA) by inoculating the broth with a single colony of a plated culture on a Luria–Bertani (LB) agar plate, and incubated overnight at 37 °C. Freshly grown *B. subtilis* cells were washed three times with phosphate buffered saline (PBS, 1X, pH 7.4) (Fisher Scientific, Pittsburgh, PA) and then re-suspended in PBS or otherwise used as stating solutions for further experimental uses.

The treatment of bacterial cells with C/TiO $_2$ hybrid dots was performed in 96-well plates. Each well was added with 150 µL bacteria cell suspension and 50 µL of the selected dot sample at desired concentrations. The final bacterial cell concentration in each well was about $\sim\!10^6\text{--}10^7$ CFU/mL, and the concentration of the hybrid dots was varied as needed while the final pH was kept constant at 7.4. Treatments with the dots at each concentration were run in triplicates. The plates were exposed to visible light (400–800 nm) from a 60 W daylight LED.

The traditional surface plating method was used to determine the viable cell numbers in the treated samples and the controls. Briefly, the bacterial samples were serially diluted (1:10) with PBS. Aliquots of 100 μL appropriate dilutions were surface-plated on LB agar plates. After incubation at 37 °C for 24 h, the colonies on the plates were counted, and the viable cell numbers were calculated in colony forming units per milliliter (CFU/mL) for all the treated samples and the controls. The logarithmic value of the reduction in viable cell number in the treated samples in comparison to the controls was used to evaluate the efficiency of bactericidal function of the C/TiO2 hybrid dots. The greater the viable cell reduction, the higher the antibacterial activity of the dots.

CRediT authorship contribution statement

Nengyu Pan: Data curation. Peter A. Okonjo: Data curation. Ping Wang: Methodology, Data curation. Yongan Tang: Software. Ya-Ping Sun: Conceptualization, Supervision. Liju Yang: Conceptualization, Supervision.

Declaration of Competing Interest

The authors declare that they have no known competing financial interests or personal relationships that could have appeared to influence the work reported in this paper.

Acknowledgment

Financial support from NSF (Grants 1701399 and 1701424) is gratefully acknowledged.

References

- [1] Y.-P. Sun, B. Zhou, Y. Lin, W. Wang, K.A.S. Fernando, P. Pathak, M.J. Meziani, B.A. Harruff, X. Wang, H. Wang, P.G. Luo, H. Yang, M.E. Kose, B. Chen, L.M. Veca, S.-Y. Xie, Quantum-sized carbon dots for bright and colorful photoluminescence, J. Am. Chem. Soc. 128 (2006) 7756–7757.
- [2] Y.-P. Sun, Fluorescent Carbon Nanoparticles, U.S. Patent 7,829,772, 2010.
- [3] L. Cao, M.J. Meziani, S. Sahu, Y.-P. Sun, Photoluminescence properties of graphene versus other carbon nanomaterials, Acc. Chem. Res. 46 (2013) 171–180.
- [4] G.E. LeCroy, S.-T. Yang, F. Yang, Y. Liu, K.A.S. Fernando, C.E. Bunker, Y. Hu, P.G. Luo, Y.-P. Sun, Functionalized carbon nanoparticles: syntheses and applications in optical bioimaging and energy conversion, Coord. Chem. Rev. 320 (2016) 66–81.
- [5] P.G. Luo, S. Sahu, S.-T. Yang, S.K. Sonkar, J. Wang, H. Wang, G.E. LeCroy, L. Cao, Y.-P. Sun, Carbon, "Quantum" dots for optical bioimaging, J. Mater. Chem. B 1 (2013) 2116–2127.
- [6] C. Ding, A. Zhu, Y. Tian, Functional surface engineering of C-dots for fluorescent biosensing and in vivo bioimaging, Acc. Chem. Res. 47 (2014) 20–30.
- [7] S.Y. Lim, W. Shen, Z. Gao, Carbon quantum dots and their applications, Chem. Soc. Rev. 44 (2015) 362–381.
- [8] V. Georgakilas, J.A. Perman, J. Tucek, R. Zboril, Broad family of carbon nanoallotropes: classification, chemistry, and applications of fullerenes, carbon dots, nanotubes, graphene, nanodiamonds, and combined superstructures, Chem. Rev. 115 (2015) 4744–4822.
- [9] K.A.S. Fernando, S. Sahu, Y. Liu, W.K. Lewis, E.A. Guliants, A. Jafariyan, P. Wang, C.E. Bunker, Y.-P. Sun, Carbon quantum dots and applications in photocatalytic energy conversion, ACS Appl. Mater. Interfaces 7 (2015) 8363–8376.
- [10] G.A.M. Hutton, B.C.M. Martindale, E. Reisner, Carbon dots as photosensitisers for solar-driven catalysis, Chem. Soc. Rev. 46 (2017) 6111–6123.
- [11] J. Du, N. Xu, J. Fan, W. Sun, X. Peng, Carbon dots for in vivo bioimaging and theranostics, Small (2019) 1805087.
- [12] T. Yuan, T. Meng, P. He, Y. Shi, Y. Li, X. Li, L. Fan, S. Yang, Carbon quantum dots: an emerging material for optoelectronic applications, J. Mater. Chem. C 7 (2019) 6820–6835.
- [13] L. Cao, K.A.S. Fernando, W. Liang, A. Seilkop, L.M. Veca, Y.-P. Sun, C.E. Bunker, Carbon dots for energy conversion applications, J. Appl. Phys. 125 (2019) 220903.
- [14] M.J. Meziani, X. Dong, L. Zhu, L.P. Jones, G.E. LeCroy, F. Yang, S. Wang, P. Wang, Y. Zhao, L. Yang, R.A. Tripp, Y.-P. Sun, Visible-light-activated bactericidal functions of carbon "Quantum" dots, ACS Appl. Mater. Interfaces 8 (2016) 10761–10766.
- [15] X. Dong, W. Liang, M.J. Meziani, Y.-P. Sun, L. Yang, Carbon dots as potent antimicrobial agents, Theranostics 10 (2020) 671–686.
- [16] Y.-P. Sun, P. Wang, Z. Lu, F. Yang, M.J. Meziani, G.E. LeCroy, Y. Liu, H. Qian, Host-guest carbon dots for enhanced optical properties and beyond, Sci. Rep. 5 (2015)

- [17] P. Anilkumar, X. Wang, L. Cao, S. Sahu, J.-H. Liu, P. Wang, K. Korch, K.N. Tackett II, A. Parenzan, Y.-P. Sun, Toward quantitatively fluorescent carbon-based "Quantum" dots, Nanoscale 3 (2011) 2023–2027.
- [18] Y. Liu, Y. Liu, H. Qian, P. Wang, G.E. LeCroy, C.E. Bunker, K.A.S. Fernando, L. Yang, M. Reibold, Y.-P. Sun, Carbon-TiO₂ hybrid dots in different configurations-optical properties, redox characteristics, and mechanistic implications, New J. Chem. 42 (2018) 10798–10806.
- [19] F. Zheng, Z. Wang, J. Chen, S. Li, Synthesis of carbon quantum dot-surface modified P25 nanocomposites for photocatalytic degradation of p-nitrophenol and acid violet 43, RSC Adv. 4 (2014) 30605–30609.
- [20] J. Wang, M. Gao, G.W. Ho, Bidentate-complex-derived TiO₂/carbon dot photo-catalysts: in situ synthesis, versatile heterostructures, and enhanced H₂ evolution, J. Mater. Chem. A 2 (2014) 5703–5709.
- [21] N.C.T. Martins, J. Ângelo, A.V. Girão, T. Trindade, L. Andrade, A. Mendes, N-doped carbon quantum dots/TiO₂ composite with improved photocatalytic activity, Appl. Catal. B-Environ. 193 (2016) 67–74.
- [22] J. Ke, X. Li, Q. Zhao, B. Liu, S. Liu, S. Wang, Upconversion carbon quantum dots as visible light responsive component for efficient enhancement of photocatalytic performance, J. Colloid. Interf. Sci. 496 (2017) 425–433.
- [23] T. Shen, Q. Wang, Z. Guo, J. Kuang, W. Cao, Hydrothermal synthesis of carbon quantum dots using different precursors and their combination with TiO₂ for enhanced photocatalytic activity, Ceram. Int. 44 (2018) 11828–11834.
- [24] M.S. Kumar, K.Y. Yasoda, D. Kumaresan, N.K. Kothurkar, S.K. Batabyal, TiO₂-Carbon Quantum Dots (CQD) nanohybrid: enhanced photocatalytic activity, Mater. Res. Express 5 (2018) 075502.
- [25] M. Li, M. Wang, L. Zhu, Y. Li, Z. Yan, Z. Shen, X. Cao, Facile microwave assisted synthesis of N-rich carbon quantum dots/dual-phase TiO₂ heterostructured nanocomposites with high activity in CO₂ photoreduction, Appl. Catal. B-Environ. 231 (2018) 269–276.
- [26] L. Ge, N. Pan, J. Jin, P. Wang, G.E. LeCroy, W. Liang, L. Yang, L.R. Teisl, Y. Tang, Y.-P. Sun, Systematic comparison of carbon dots from different preparations-consistent optical properties and photoinduced redox characteristics in visible spectrum and structural and mechanistic implications, J. Phys. Chem. C 122 (2018) 21667–21676.
- [27] Z. Li, Y. Fang, X. Zhan, S. Xu, Facile Preparation of squarylium dye sensitized TiO₂ nanoparticles and their enhanced visible-light photocatalytic activity, J. Alloys Compd. 564 (2013) 138–142.
- [28] X. Li, J.-L. Shi, H. Hao, X. Lang, Visible light-induced selective oxidation of alcohols with air by dye-sensitized TiO₂ photocatalysis, Appl. Catal. B-Environ. 232 (2018) 260–267.
- [29] P. Chowdhury, J. Moreira, H. Gomaa, A.K. Ray, Visible-solar-light-driven photocatalytic degradation of phenol with dye-sensitized TiO₂: parametric and kinetic study. Ind. Eng. Chem. Res. 51 (2012) 4523–4532.